

# Ultra-short period contact binaries: restricting the parameters of the primary using Gaia parallax

Alexander Kurtenkov<sup>1</sup>

Institute of Astronomy and NAO, Bulgarian Academy of Sciences,  
72 Tsarigradsko Shose Blvd., BG-1784, Sofia, Bulgaria  
al.kurtenkov@gmail.com

(Submitted on 20.08.2021; Accepted on 02.12.2021)

**Abstract.** Possible M-type contact binaries were investigated by selecting W UMa-type variables with orbital periods below the 0.22-day cutoff. Gaia parallaxes were combined with Gaia and 2MASS photometry to obtain G and J-band absolute magnitudes of 674 red variable stars catalogued as contact binaries in the VSX database. The absolute magnitude of main sequence cool dwarfs varies strongly with spectral type, which was used to create a selection of 218 systems with primaries potentially of spectral types M0-M3. Lightcurves of the 46 systems with lowest near-infrared luminosities were inspected individually to confirm or reject the W UMa classification where possible. The extinction limits and amplitudes were combined with the calculated absolute magnitudes in order to set upper limits for the masses of the primary components. This is achieved via the consideration that the luminosity of the primary is no less than that of a main sequence star of the same mass. For 26 possible contact binaries the mass of the primary was limited to less than 0.5 solar masses with some systems having upper limits for the primary as low as 0.35 solar masses. These rare systems are intriguing targets for more detailed observations since they are on the low-mass end of the contact binary distribution and their formation and evolution are still unclear.

**Key words:** binaries: eclipsing – catalogs

## 1. Introduction and rationale

Contact binary systems are predominantly of spectral types F, G, and K. They are usually observed as variable stars of the W UMa-type: eclipsing variables whose lightcurves present round-shaped maxima as well as primary and secondary minima of similar depths due to the small temperature difference of the components. Notable models explaining the W UMa lightcurves as caused by eclipses in contact binary systems include those by Lucy (1968) and Rucinski (1993). Two main W UMa subtypes are defined (Binnendijk 1970) – the A-subtype, usually consisting of A and F spectral type components, and the W-subtype, which have G and K type components and, respectively, shorter orbital periods. Only a few confirmed M-type contact binaries have been discovered and even fewer of these are well-studied (Latković et al. 2021). The period distribution of contact binaries has a sharp cut-off at  $P = 0.22$  d (Rucinski 1992). As M-dwarfs have the lowest radii on the stellar main sequence, M-type systems are expected to have the lowest semi-major axes and, respectively, the shortest periods among contact binaries. Due to the rarity of these M-type systems, variables, classified as W UMa-type binaries below the 0.22-day period cut-off are of great interest. It is still an open question why these M-type binaries are so rare even after accounting for the selection bias caused by their low luminosity. Jiang et al. (2012) suggest that systems with a primary component mass below  $0.63 M_{\odot}$  are dynamically unstable upon activation of the mass transfer through  $L_1$ , which hinders the formation of a durable low-mass contact binary. This consideration elevates the interest specifically in systems with low-mass primaries.

The current work aims to select possible M-type contact binaries with low-mass primaries for further, more detailed studies. The number of known contact binaries has considerably increased thanks to recent variability surveys, most importantly, the Zwicky Transient Facility (Chen et al. 2020). Meanwhile, the Gaia mission (Gaia Collaboration et al. 2021) has supplied parallax data for systems at a distance of the order of 1 kpc with an unprecedented reliability. As M-type discoveries are expected at low distances due to their low luminosities, Gaia data combined with other photometry can be used to calculate approximate absolute magnitudes. The absolute magnitudes vary strongly for M-dwarfs – the typical difference between M0V and M5V is 3.1 mag in J-band and 4.3 mag in Gaia G-band (Pecaut & Mamajek 2013). Thus, these absolute magnitudes can be used to set an upper limit of the luminosity and spectral type of the primary – the extremal case being if the luminosity of the secondary is negligible. As there is no reason for the primary to be less luminous than a single main sequence star of the same mass, an upper limit of the mass can also be estimated. It is hereby suggested that this is a decent method to restrict the parameters of the M-type primary, whereas colors are more strongly influenced by the uncertainties due to the amplitude of the eclipses and the interstellar extinction relative to their differences between spectral subtypes.

## 2. Object selection

As of 2021 the Variable Star Index (VSX<sup>1</sup>) lists 2489 objects, classified as W UMa-type variables. The following criteria were used when matching these to the Gaia EDR3 catalog:

- Relative Gaia parallax error  $e\_Plx/Plx < 0.2$
- Gaia  $RP$  magnitude error  $e\_RPmag < 0.1$
- Gaia color  $G - RP > 0.8$

The latter value has been chosen as the typical value for type M0V is  $G - RP = 0.9$ , whereas the other criteria are liberal. A total of 688 matches were found. These were matched with the 2MASS catalog in order to include the  $J$ -band magnitudes. The only criterion was the error in  $J$ -band magnitude  $e\_Jmag < 0.2$ . This left us with 674 objects. A search radius of  $5''$  was used for all matches.

Initial absolute magnitudes (uncorrected for extinction) were calculated by applying the distance moduli calculated from the Gaia parallax  $p$  via:

$$M_G = G + 5 \lg(p[\text{mas}]) - 10 \quad (1)$$

$$M_J = J + 5 \lg(p[\text{mas}]) - 10 \quad (2)$$

Although it would be difficult to determine the actual extinction, the maximum values can be set at the galactic line-of-sight extinction as calculated by Schlafly & Finkbeiner (2011). As these are maximum values, they are not applied to the absolute magnitudes, but they are presented next to the results for consideration. A major advantage of using the 2MASS  $J$ -band magnitudes is the low extinction in the near infrared.

**Table 1.** Typical parameters of main sequence M-dwarfs.

Spectral type	$T_{eff}$	$R/R_\odot$	Mass [ $M_\odot$ ]	$BP - RP$	$M_G$	$M_J$
M0V	3850	0.588	0.57	1.84	8.16	5.97
M0.5V	3770	0.544	0.54	1.97	8.44	6.19
M1V	3660	0.501	0.50	2.09	8.82	6.48
M1.5V	3620	0.482	0.47	2.13	8.98	6.59
M2V	3560	0.446	0.44	2.23	9.29	6.81
M2.5V	3470	0.421	0.40	2.39	9.67	7.01
M3V	3430	0.361	0.37	2.50	10.05	7.38
M3.5V	3270	0.300	0.27	2.78	10.87	7.93
M4V	3210	0.274	0.23	2.94	11.21	8.20
M4.5V	3110	0.217	0.18	3.16	12.04	8.80
M5V	3060	0.196	0.16	3.35	12.45	9.09
M5.5V	2930	0.156	0.12	3.71	13.35	9.72
M6V	2810	0.137	0.10	4.16	14.26	10.18
M6.5V	2740	0.126	0.09	4.50	14.40	10.47
M7V	2680	0.120	0.09	4.65	14.72	10.70

Typical parameters of main sequence M-dwarfs after Pecaut & Mamajek (2013), supplemented online<sup>2</sup> were used to set a limit for the spectral type of the primary component. The values are presented in Table 1. A list of possible M-type contact binaries was selected based on these values by applying the following criteria:

- Absolute  $G$ -band magnitude  $M_G > 8.2$
- Absolute  $J$ -band magnitude  $M_J > 6.0$
- Gaia color  $BP - RP > 1.9$

<sup>1</sup> <https://www.aavso.org/vsx/>

<sup>2</sup> [https://www.pas.rochester.edu/~emamajek/EEM\\_dwarf\\_UBVIJHK\\_colors\\_Teff.txt](https://www.pas.rochester.edu/~emamajek/EEM_dwarf_UBVIJHK_colors_Teff.txt)

This selection contains 218 systems, which are of significant interest for further observations and analysis, e.g. lightcurve modeling. The majority of these systems, if they have been classified correctly, are expected to contain a primary less massive than  $0.6M_{\odot}$ . The cutoff values of the absolute magnitude distributions ( $\approx 7.5$  for  $M_J$  and  $\approx 10$  for  $M_G$ , Fig. 1) suggest that almost all of these systems are of spectral type earlier than M3.5V, so masses of the primaries below  $\approx 0.3M_{\odot}$  should be extremely rare if there are any.

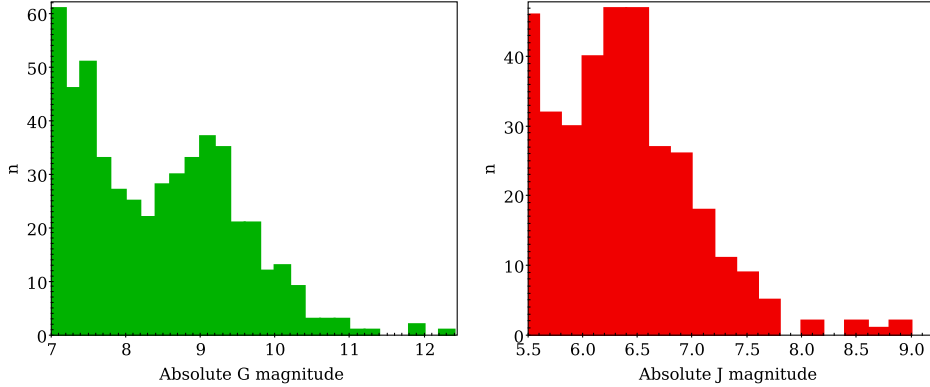


**Fig. 1.** Absolute magnitude distribution in  $G$  and  $J$ -band using 0.2 mag bins. Not corrected for extinction.

The orbital periods of the selected systems are plotted versus distance on Fig. 2. It shows that the selected systems have statistically shorter periods, as their radii are smaller. Due to their low luminosities almost all of them are within 1 kpc from the Earth, whereas many systems from the initial selection are located farther.

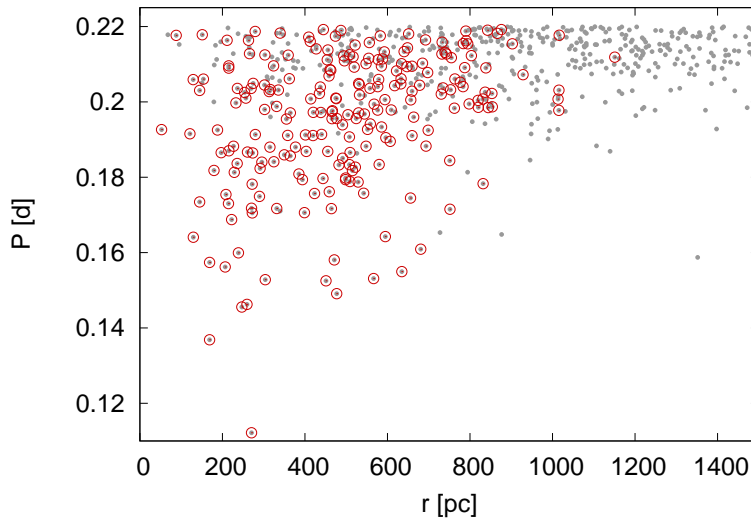


**Fig. 2.** A distance-period diagram for all 674 systems (small grey circles). The selected 218 systems (large hollow red circles) are statistically closer to the Earth as their luminosities are lower and they include most of the systems with the shortest periods.

The full table containing coordinates, lightcurve parameters and magnitudes of the catalog matches for all systems is available upon request from the author.

### 3. Objects near the low-mass end

The selection contains 46 objects with  $M_J > 7.0$ , which should be near the low-mass end. These objects are presented in Table 2 with their amplitudes  $A$  and periods  $P$  according to VSX and their Gaia parallaxes  $p$  and  $BP - RP$  colors. Each of them was individually considered as an object of interest.

**Table 2.** The list of selected M-type contact binary candidates with the lowest  $J$ -band luminosity: parameters from VSX and Gaia.

Name	RA (J2000)	Dec (J2000)	$A$ [mag]	$P$ [d]	$p$ [mas]	$\sigma_p$	$BP - RP$
ZTF J024005.10+513845.5	40.0212548	51.64594	0.409	0.1599	4.187	0.835	2.57
WTS 19b-3-06008	293.455638	36.90054	0.08	0.1121	3.697	0.493	2.57
CSS J093044.8+264957	142.686717	26.83252	0.2	0.1970	2.742	0.484	2.01
ZTF J150926.26+583628.1	227.359485	58.60779	0.161	0.1734	6.911	0.057	2.78
ZTF J001012.42+452925.1	2.55179707	45.49026	0.179	0.1836	4.243	0.116	2.57
ZTF J213409.46+335033.8	323.539439	33.84273	0.534	0.2095	4.644	0.346	2.45
ZTF J191844.32+532028.2	289.684684	53.34113	0.289	0.1717	3.016	0.085	2.40
ZTF J233629.58+505049.5	354.123284	50.84707	0.153	0.1818	5.570	0.060	3.08
ZTF J204919.36+080812.0	312.330697	8.136691	0.142	0.1910	2.791	0.265	2.13
ZTF J175927.14+654540.4	269.863068	65.76120	0.579	0.1527	3.292	0.109	2.76
CSS J234019.3+122438	355.080936	12.41074	0.35	0.1368	5.924	0.056	2.36
ZTF J174317.23+401313.1	265.821783	40.22024	0.718	0.1490	2.096	0.202	2.51
ZTF J145410.58+314216.2	223.544137	31.70448	0.232	0.2060	6.503	0.051	2.68
ZTF J193121.28+293951.2	292.838716	29.66423	0.293	0.1580	2.122	0.174	2.72
ZTF J051637.22+380939.8	79.1544408	38.16008	0.234	0.2043	1.475	0.256	1.97
ZTF J220421.03+163655.8	331.087656	16.61549	0.243	0.1748	3.452	0.130	2.99
ZTF J174214.33+642525.0	265.559742	64.42358	0.283	0.2025	3.941	0.062	2.75
ZTF J182843.57+372540.6	277.181579	37.42795	0.28	0.2131	1.351	0.174	2.21
ZTF J011509.92+130340.9	18.7913604	13.06135	0.462	0.1549	1.575	0.267	2.07
ZTF J015312.72+444309.8	28.3029965	44.71939	0.4	0.1754	4.793	0.099	2.87
ZTF J003651.36+503617.7	9.21400193	50.60490	0.414	0.1788	1.964	0.173	2.61
ZTF J175432.47+373447.6	268.635354	37.57988	0.221	0.1925	5.315	0.047	2.90
ZTF J053128.93+512221.6	82.8705820	51.37263	0.41	0.1959	1.507	0.261	2.25
CSS J082958.5+355923	127.494109	35.98983	0.22	0.1455	4.050	0.095	2.71
ZTF J011434.64+622754.1	18.6443964	62.46503	0.181	0.1705	3.671	0.067	2.65
ZTF J221742.28+485418.4	334.426184	48.90513	0.156	0.1954	2.816	0.088	2.67
ZTF J183104.30+712050.5	277.767912	71.34735	0.157	0.1879	3.172	0.065	2.39
CSS J111647.8+294602	169.199264	29.76744	0.3	0.1462	3.852	0.080	2.47
ZTF J001725.54+513930.3	4.35645188	51.65844	0.348	0.2008	2.101	0.156	2.69
2MASS J08115860+3119595	122.994093	31.33335	0.3	0.1561	4.839	0.050	2.26
ZTF J112409.81+314128.5	171.040919	31.69124	0.293	0.1913	2.271	0.192	2.62
CSS J224134.8+253648	340.395580	25.61351	0.29	0.1573	5.928	0.064	2.86
CSS J030238.1-065034	45.6587354	-6.84290	0.19	0.2128	3.766	0.086	2.87
CSS J001242.4+130809	3.17693974	13.13583	0.24	0.1640	7.730	0.047	2.87
ZTF J184257.77-014740.2	280.740741	-1.79452	0.422	0.1705	2.508	0.142	2.70
ZTF J191410.07+322037.4	288.542008	32.34370	0.208	0.2048	1.886	0.125	2.31
ZTF J134037.03+733037.0	205.154323	73.51027	0.266	0.1793	2.006	0.1	2.24
ZTF J202921.75+115328.4	307.340661	11.89123	0.571	0.2005	1.523	0.241	2.54
ZTF J223934.51+200033.8	339.893820	20.00940	0.308	0.1910	2.383	0.175	2.78
ZTF J210046.30+420324.7	315.192950	42.05683	0.276	0.2040	1.735	0.166	2.61
ZTF J055824.63+252036.2	89.6026576	25.34337	0.394	0.1530	1.766	0.188	2.55
CSS J081001.0+324429	122.504424	32.74127	0.35	0.1865	1.964	0.148	2.29
ZTF J215438.54+655322.6	328.660633	65.88961	0.273	0.1868	2.482	0.080	2.63
ZTF J165835.01+225905.7	254.645883	22.98490	0.317	0.1761	2.178	0.112	2.75
ZTF J135005.20+501920.7	207.521691	50.32240	0.156	0.2048	3.643	0.052	2.39
ZTF J204646.04+233929.0	311.691841	23.65805	0.546	0.1840	3.382	0.076	2.26

The absolute magnitudes and other results for these systems are presented in Table 3. In order to calculate the absolute magnitude errors, the error propagation of both the magnitudes and parallaxes had to be taken into account. The errors in the distance moduli caused by the parallax uncertainties  $\sigma_p$  were calculated and applied via:

$$\sigma_{m-M} = \sigma(-5 \lg(p'') - 5) \approx \frac{5}{\ln(10)} \frac{\sigma_p}{p} \quad (3)$$

$$\sigma_{M_G}^2 = \sigma_{m-M}^2 + \sigma_G^2 \quad (4)$$

$$\sigma_{M_J}^2 = \sigma_{m-M}^2 + \sigma_J^2 \quad (5)$$

The total galactic line-of-sight extinctions  $A_r$  and  $A_J$  were manually checked with the NED extinction calculator<sup>3</sup>. The SDSS  $r$  filter has a central wavelength close to the Gaia  $G$  filter ( $\approx 600$  nm). However, all selected objects are red, so they emit predominantly in the red region of the wide  $G$ -band, where the extinction is lower than in the center. So we can safely assume that the extracted  $r$ -band extinction values are upper limits, i.e.  $A_G < A_r$ .

As many of these objects are faint (18-20 mag), there is a considerable risk of incorrect automatic classification of their variability type. Therefore each individual lightcurve was visually inspected. Comments of the variability types based on these manual inspections are also included in Table 3. The AAVSO VSX variability type designations are used for this purpose (EA = Algol (possibly with strong ellipsoidal effects), EB =  $\beta$  Lyr, EW = W UMa, ELL = rotating ellipsoidal variable). It appears that the VSX classification is false in at least 9 of the 46 cases and, possibly, in more than half of them.

The upper limits for the mass of the primary component, presented in the final column, are calculated as the lesser of the two main sequence masses, corresponding to  $M_{Gmax}$  and  $M_{Jmax}$ , where:

$$M_{Gmax} = M_G - 2\sigma_{M_G} - A - A_r \quad (6)$$

$$M_{Jmax} = M_J - 2\sigma_{M_J} - A - A_J \quad (7)$$

The absolute magnitudes and masses are compared to interpolated values from Table 1.

These are almost worst-case-scenario absolute magnitude values – the amplitudes  $A$  are subtracted in case the  $G$  and  $J$ -band estimates are made near a minimum, and maximum extinctions are considered, although most systems are nearby (Fig. 2). Since coefficients of 2 are used for taking the absolute magnitude errors into account, these upper limits are set with a  $\sim 95\%$  confidence, i.e. a roughly normal probability distribution is assumed for the absolute magnitudes and for the mass of the primary. These mass limits are calculated only for the systems, whose lightcurves correspond to a W UMa-type, and are valid only in case the systems actually are contact binaries. A total of 26 systems in Table 3 are expected to have a primary component less massive than  $0.5M_\odot$ .

## Summary

The absolute magnitudes of main sequence M-dwarfs are very sensitive of their masses. The primary components in contact binary systems are expected to have a luminosity not lower than that of a main sequence star with the same mass. Thus we can set an upper limit of the mass of the primary only from the absolute magnitude of the system. This is especially useful in the search for M-type contact binaries since most of these objects are faint and difficult to observe spectroscopically. This paper aims to present such an approach for selecting promising targets for more detailed exploration. By combining Gaia parallaxes with Gaia and 2MASS photometry we selected a total of 218 systems below the 0.22 d period cutoff as potential M-type contact binaries. A smaller subselection of 46 of these systems was manually inspected – the classification of their lightcurves was checked and the masses of the primaries were limited. Future targeted observations of these systems will show their exact location on the low-mass end of the distribution of contact binary systems and how they got there.

<sup>3</sup> [https://ned.ipac.caltech.edu/extinction\\_calculator](https://ned.ipac.caltech.edu/extinction_calculator)

**Table 3.** The list of selected M-type contact binary candidates with the lowest  $J$ -band luminosity: calculated absolute magnitudes (uncorrected for extinction), maximum extinction values, lightcurve classification and upper limits for the mass of the primary.

Name	$M_G$	$\sigma_{M_G}$	$M_J$	$\sigma_{M_J}$	$A_r$	$A_J$	lightcurve	$M_{1max}[M_\odot]$
ZTF J024005.10+513845.5	12.22	0.43	8.977	0.43	0.71	0.22	noisy	< 0.35
WTS 19b-3-06008	11.99	0.29	8.620	0.29	0.40	0.12	EW	< 0.32
CSS J093044.8+264957	10.80	0.38	8.410	0.39	0.05	0.02	EW	< 0.37
ZTF J150926.26+583628.1	11.12	0.01	8.110	0.03	0.02	0.01	EA/EB	-
ZTF J001012.42+452925.1	10.78	0.05	8.092	0.07	0.18	0.06	noisy/sparse	< 0.33
ZTF J213409.46+335033.8	10.82	0.16	7.748	0.16	0.40	0.13	EB	-
ZTF J191844.32+532028.2	10.37	0.06	7.657	0.07	0.22	0.07	EA/EB	-
ZTF J233629.58+505049.5	10.77	0.02	7.657	0.03	0.44	0.14	noisy/sparse	< 0.36
ZTF J204919.36+080812.0	10.31	0.20	7.629	0.21	0.17	0.05	EB/EW	< 0.40
ZTF J175927.14+654540.4	10.69	0.07	7.626	0.08	0.11	0.04	EB	-
CSS J234019.3+122438	10.19	0.02	7.586	0.03	0.12	0.04	EW/ELL	< 0.39
ZTF J174317.23+401313.1	10.80	0.20	7.575	0.22	0.08	0.03	EA/EB	-
ZTF J145410.58+314216.2	10.42	0.01	7.568	0.02	0.04	0.01	EA/EB	-
ZTF J193121.28+293951.2	10.33	0.17	7.516	0.19	1.32	0.41	EW	< 0.51
ZTF J051637.22+380939.8	9.382	0.37	7.491	0.40	1.83	0.57	EW	< 0.58
ZTF J220421.03+163655.8	10.40	0.08	7.476	0.08	0.12	0.04	EW	< 0.39
ZTF J174214.33+642525.0	10.38	0.03	7.450	0.04	0.08	0.03	EA/EB	-
ZTF J182843.57+372540.6	9.637	0.28	7.426	0.31	0.11	0.04	EB/EW	< 0.50
ZTF J011509.92+130340.9	9.743	0.36	7.388	0.39	0.08	0.03	EW	< 0.54
ZTF J015312.72+444309.8	10.36	0.04	7.372	0.05	0.17	0.05	EW	< 0.40
ZTF J003651.36+503617.7	10.11	0.19	7.351	0.20	0.38	0.12	noisy/sparse	< 0.48
ZTF J175432.47+373447.6	10.39	0.01	7.344	0.03	0.09	0.03	EW	< 0.37
ZTF J053128.93+512221.6	9.990	0.37	7.308	0.38	0.84	0.26	EW/ELL	< 0.53
CSS J082958.5+355923	10.35	0.05	7.287	0.05	0.10	0.03	EW/ELL	< 0.38
ZTF J011434.64+622754.1	10.17	0.03	7.275	0.05	3.54	1.10	EW	< 0.58
ZTF J221742.28+485418.4	10.08	0.06	7.237	0.07	0.67	0.21	EW/ELL	< 0.45
ZTF J183104.30+712050.5	10.06	0.04	7.226	0.05	0.12	0.04	noisy	< 0.40
CSS J111647.8+294602	10.02	0.04	7.219	0.05	0.04	0.01	EW/ELL	< 0.42
ZTF J001725.54+513930.3	10.02	0.16	7.213	0.17	0.38	0.12	EW/ELL	< 0.48
2MASS J08115860+3119595	9.579	0.02	7.186	0.03	0.09	0.03	EB/EW	< 0.44
ZTF J112409.81+314128.5	9.969	0.18	7.158	0.18	0.04	0.01	EW	< 0.45
CSS J224134.8+253648	10.37	0.02	7.154	0.03	0.11	0.03	EW/ELL	< 0.38
CSS J030238.1-065034	10.05	0.05	7.123	0.06	0.18	0.05	EW	< 0.42
CSS J001242.4+130809	10.07	0.01	7.118	0.02	0.19	0.06	EB/EW	< 0.41
ZTF J184257.77-014740.2	10.05	0.12	7.117	0.14	7.58	2.35	EW	< 0.70
ZTF J191410.07+322037.4	9.865	0.14	7.085	0.16	0.40	0.13	noisy	< 0.48
ZTF J134037.03+733037.0	9.515	0.10	7.082	0.12	0.04	0.01	EB/EW	< 0.47
ZTF J202921.75+115328.4	9.933	0.34	7.080	0.35	0.21	0.07	EB	-
ZTF J223934.51+200033.8	10.11	0.16	7.070	0.16	0.08	0.03	EW	< 0.44
ZTF J210046.30+420324.7	10.04	0.20	7.068	0.22	3.10	0.96	EW	< 0.67
ZTF J055824.63+252036.2	9.781	0.23	7.067	0.24	2.61	0.81	EW	< 0.67
CSS J081001.0+324429	9.592	0.16	7.066	0.17	0.13	0.04	EW/ELL	< 0.52
ZTF J215438.54+655322.6	9.857	0.07	7.064	0.08	1.36	0.42	EA/EB	-
ZTF J165835.01+225905.7	9.996	0.11	7.051	0.12	0.17	0.05	EB/EW	< 0.45
ZTF J135005.20+501920.7	9.664	0.03	7.019	0.04	0.03	0.01	EB/EW	< 0.45
ZTF J204646.04+233929.0	9.756	0.04	7.010	0.05	0.36	0.11	EW	< 0.51

## Acknowledgements

This work has made use of data from the European Space Agency (ESA) mission *Gaia* (<https://www.cosmos.esa.int/gaia>), processed by the *Gaia* Data Processing and Analysis Consortium (DPAC<sup>4</sup>). Funding for the DPAC has been provided by national institutions, in particular the institutions participating in the *Gaia* Multilateral Agreement. This work was supported by the Bulgarian Ministry of Education and Science under the National Research Programme "Young scientists and postdoctoral students" approved by DCM #577/17.08.2018.

## References

- [Binnendijk, L., 1970, *Vistas in Astronomy*, 12, 217  
 [Chen, X., Wang, S., Deng, L., de Grijs, R., Yang, M., Tian, H., 2020, *The Astrophysical Journal Supplement Series*, 249, 18

<sup>4</sup> <https://www.cosmos.esa.int/web/gaia/dpac/consortium>

- Gaia Collaboration et al., 2021, *Astronomy & Astrophysics*, 649, A1
- Jiang, D., Han, Z., Ge, H., Yang, L., Li, L., 2012, *MNRAS*, 421, 2769
- Latković, O., Čeki, A., Lazarević, S., 2021, *The Astrophysical Journal Supplement Series*, 254, 10
- Lucy, L. B., 1968, *Astrophysical Journal*, 153, 877
- Pecauc, M. J., Mamajek, E. E., 2013, *The Astrophysical Journal Supplement*, 208, 9
- Rucinski, S. M., 1992, *Astronomical Journal*, 103, 960
- Rucinski, S. M., 1993, *Publications of the Astronomical Society of the Pacific*, 105, 1433
- Schlafly, E. F., Finkbeiner, D. P., 2011, *The Astrophysical Journal*, 737, 103